Journal of Applied Polymer Science

Nanocomposites of Poly(propylene carbonate) Reinforced with Cellulose Nanocrystals via Sol-Gel Process

Xinhang Wang, Yumin Xia, Peng Wei, Yuwei Chen, Yanping Wang, Yimin Wang
State Key Laboratory for Modification of Chemical Fibers and Polymer Materials, College of Materials Science and Engineering, Donghua University, Shanghai 201620, People's Republic of China
Correspondence to: Y. Wang (E-mail: ymw@dhu.edu.cn)

ABSTRACT: Cellulose nanocrystals (CNCs) organogels were first produced from aqueous dispersion through solvent exchange of CNCs to acetone via a simple sol-gel process. After mixing the organogels with poly(propylene carbonate) (PPC) in dimethylformamide followed by solution casting, green nanocomposites were obtained with CNCs well dispersed in PPC polymer matrix which was confirmed by scanning electron microscopy observations. Differential scanning calorimeter analysis revealed that glass transition temperature of the nanocomposites was slightly increased from 34.0 to 37.4°C. Tensile tests indicated that both yield strength and Young's modulus of CNCs/PPC nanocomposites were doubled by adding 10 wt % CNCs. However, poor thermal stability of PPC occurred after incorporating with CNCs due to the thermo-sensitive sulfate groups located on the surface of CNCs. Furthermore, PPC became more hydrophilic because of the inclusion of CNCs according to the water contact angle measurement. The enhanced mechanical and hydrophilic properties, coupled with the inherent superior biocompatibility and degradability, offered CNCs/PPC composites potential application in biomedical fields. © 2014 Wiley Periodicals, Inc. J. Appl. Polym. Sci. **2014**, *131*, 40832.

KEYWORDS: cellulose; composites; nanocrystals; poly(propylene carbonate); sol-gel process

Received 10 February 2014; accepted 7 April 2014
DOI: 10.1002/app.40832

INTRODUCTION

In response to the emerging environmental problems caused by the heavy use of non-degradable polymer materials, biodegradable, and renewable polymers had been extensively investigated and developed worldwide in recent years.[1,2] Poly(propylene carbonate) (PPC) is a kind of aliphatic polycarbonate, which not only possesses wonderful biodegradability but also contributes to reducing the greenhouse effect due to the utilization of CO_2 as one of reaction components.[3] PPC has a wide range of potential applications such as packaging materials, adhesives, and elastomers.[4,5] However, PPC is an amorphous polymer with very low glass transition temperature and relative poor mechanical properties. To improve the mechanical performances and thus extend the practical application of PPC, multi-walled carbon nanotubes,[6] graphite oxide,[7,8] montmorillonite,[9] and glass fiber[10] had been composited with PPC; however, those inorganic fillers are not biodegradable which may limit the development of PPC in biomedical field.

Cellulose is the most abundant biomass material in nature, with approximately 5×10^{11} tons being generated yearly. When cellulose fibers are subjected to acid hydrolysis, its disordered regions will be removed. At the same time, the fibers release the rigid crystalline regions which form needle-shaped nanoparticles of cellulose nanocrystals (CNCs). Because of the fully stretched cellulose chains in perfect crystals, CNCs own outstanding mechanical performances with high Young's modulus (150 GPa) and strength (7 GPa),[1] therefore, CNCs had been frequently chosen as reinforcing material for various polymers such as polylactide,[11] cellulose acetate butyrate,[12,13] poly(butylene succinate),[14] poly(vinyl alcohol),[15] poly(3-hydroxybutyrate-*co*-3-hydroxyvalerate),[16] polyurethane,[17] and alginate.[18]

CNCs are difficult to be well re-dispersed because of its strong tendency to aggregate during the drying process. Even so, stable CNCs suspension can be prepared in several organic solvents such as DMF, DMSO, and NMP,[19–21] but this re-dispersing process involved expensive lyophilization and extensive ultrasonication which can cause morphology damage, leading to decrease in mechanical performance of the CNCs.[21] Hence, surface modification via reaction of the hydroxyl groups had been mostly used to improve the dispersion of CNCs in the polymer matrix. However, the reinforcing effect might be restricted with the suppressed desirable interactions between CNCs, which were often claimed to be responsible for the formation of a percolating hydrogen-bonded network in nanocomposites.[22] Recently, a solvent-exchange method was widely adopted to get well dispersed CNCs in organic solvents from aqueous phase.[12,23–25]

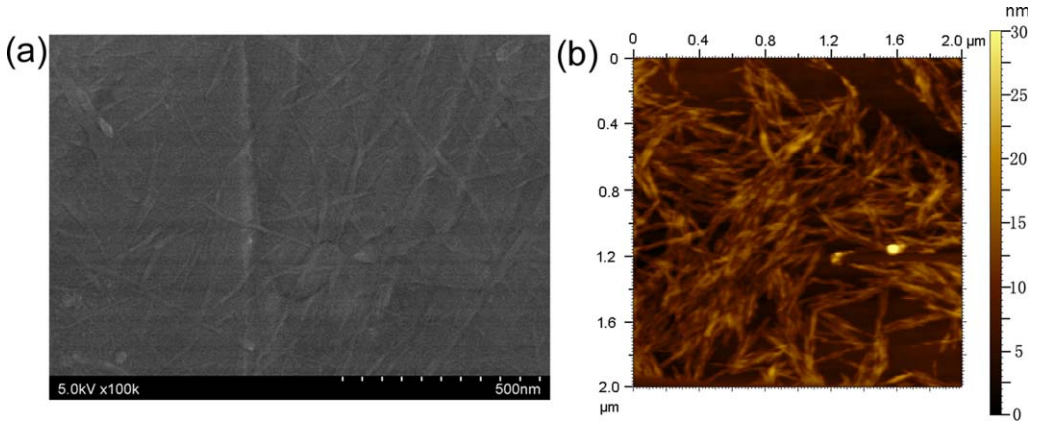

Figure 1. The (a) SEM and (b) AFM images of CNCs. [Color figure can be viewed in the online issue, which is available at wileyonlinelibrary.com.]

Inspired by the report that homogeneous polymer/nanofiber composites were prepared based on the formation of a three-dimensional template of well-individualized nanofibers via a sol-gel process,[24] Siqueira and Tang took advantage of the sol-gel process as a solvent exchange method to achieve well dispersion of CNCs in cellulose acetate butyrate[12] and epoxy resin,[26] respectively. To the best knowledge, there were two publications concerned with PPC reinforced with CNCs. Hu et al.[27] added CNCs suspensions into the PPC/THF solution and then PPC/CNCs powder was obtained and injection molded after coagulating in a large amount of methanol. Wang et al.[28] reported well dispersion of CNCs in PPC matrix using the re-dispersible CNCs powder whose preparation involved a complicated supercritical extraction process.

In this work, with the aim to reinforce PPC with biodegradable nanofillers, CNCs were incorporated into PPC using a simple sol-gel approach along with a solution casting technique. The hydrophilicity, thermal, and mechanical properties of a sequence of CNCs/PPC nanocomposites with 1–10 wt % CNCs content were studied to understand the reinforcing mechanism.

EXPERIMENTAL

Materials

PPC was provided from Melic Sea High-tech Group Company (Inner Mongolia, China, M_n: 100 K). Microcrystalline cellulose (MCC, particle size about 50 μm), commercially available as CEOLUS™, was kindly provided by Asahi Kasei. Sulfuric acid (98%), acetone (99%), and DMF (98%) were purchased from Sinopharm Chemical Reagent and used as received.

Preparation of CNCs

CNCs were prepared using the following procedure: 8.7 g MCC was mixed with 100 mL 64 wt % sulfuric acid solution. The MCC/sulfuric acid suspension was then put in a water bath and vigorously stirred at 50°C for 90 min under ultrasonic treatment. The resultant suspension was repeatedly rinsed with deionized water and centrifuged until the supernatant became turbid. The concentration of final CNCs dispersion was approximately 3.0 mg/mL.

CNCs Organogels

CNCs–acetone organogels were fabricated from aqueous dispersion of CNCs using a sol-gel process previously reported by Capadona et al.[24] After defoaming, CNCs suspension (50 mL, 3 mg/mL) was gently added with acetone (200 mL) to form an organic layer on the top of the aqueous layer. The acetone layer was exchanged twice a day and could be agitated occasionally to facilitate solvent exchange until the mechanically coherent CNCs–acetone organogels were formed in 4–5 days and kept at 4°C until use. The organogels were weighted in their swollen and dried state and the CNCs to total weight ratio was determined as an average of three independent samples.

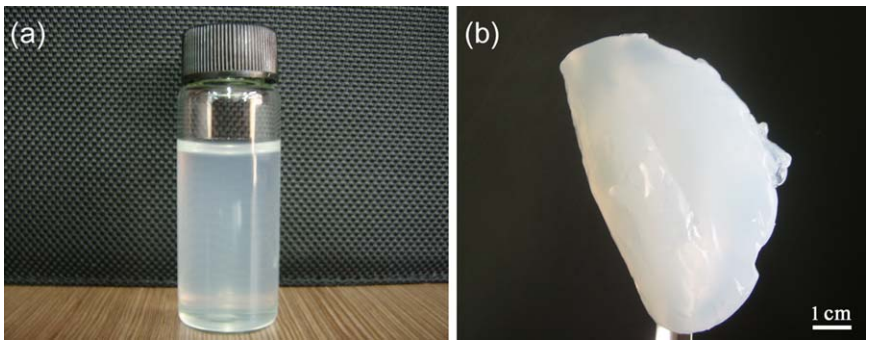

Figure 2. Photographs of (a) dispersion of as-prepared CNCs in water and (b) organogels prepared from CNCs in acetone. [Color figure can be viewed in the online issue, which is available at wileyonlinelibrary.com.]

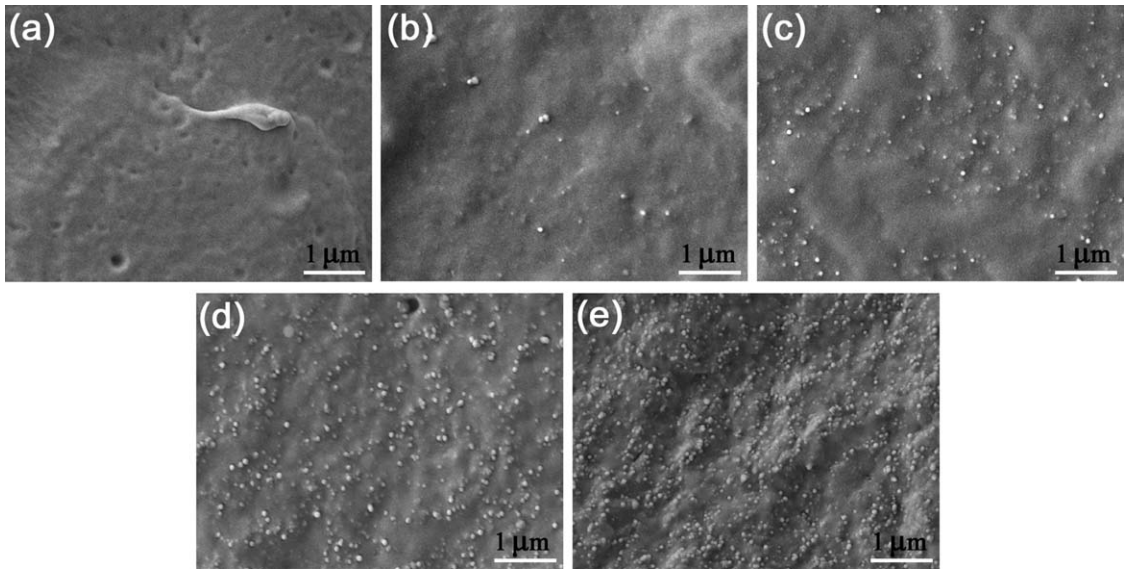

Figure 3. SEM micrographs of fractured cross sections of (a) PPC and CNCs/PPC nanocomposites with (b) 1 wt %, (c) 3 wt %, (d) 5 wt %, and (e) 10 wt % CNCs.

Processing of CNCs/PPC Nanocomposites

PPC/DMF solution (2.5 w/v%) was prepared and added with a certain amount of CNCs–acetone organogels to obtain CNCs/PPC nanocomposites with varying content of CNCs at 0, 1, 3, 5, and 10 wt %. When the organogels were introduced into PPC/DMF solution, they were disappeared and re-dispersed upon gentle shaking in several minutes. The residual acetone in DMF was evaporated using a rotary evaporator. The CNCs/PPC suspension was cast on glass slides and dried in vacuum oven at 60°C for 72 h. At last, the nanocomposites films with thickness of 100 μm were obtained.

Characterization

The morphology of CNCs was observed on a field emission scanning electron microscopy (FE-SEM, HITACHI S-4800) and an atomic force microcopy (AFM, Agilent5500). The dispersion of CNCs in CNCs/PPC nanocomposites was evaluated by FE-SEM.

Mechanical properties of neat PPC and the nanocomposites films were investigated on an electronic universal testing machine (Kexin WDW3020) at 15°C. The size of tailored rectangular shape test specimens was 40 mm × 5 mm × 0.1 mm and 30 mm in gauge length. The test was performed at a constant tensile rate of 40 mm/min. The data provided were the average values based on at least eight measurements.

Thermogravimetric analysis (TA Q5000IR) was conducted from 50 to 600°C with the heating rate of 20°C/min at a nitrogen current of 50 mL/min.

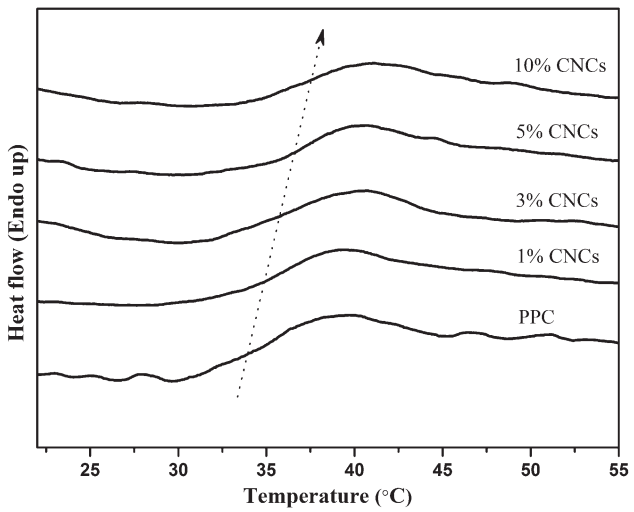

Figure 4. DSC curves of neat PPC and its nanocomposites with various CNCs content.

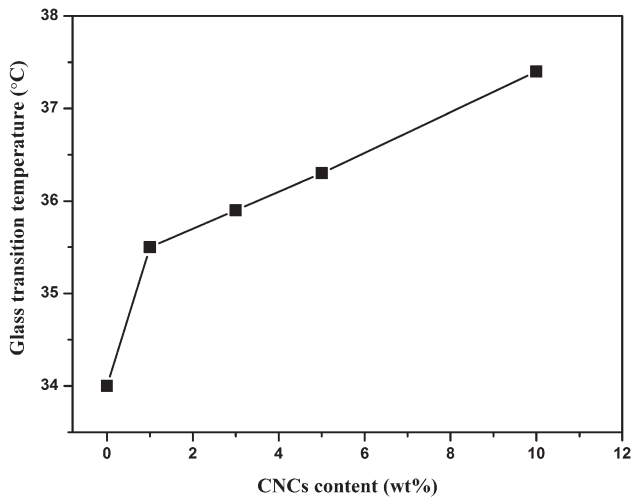

Figure 5. The T_g of CNCs/PPC nanocomposites as a function of CNCs content.

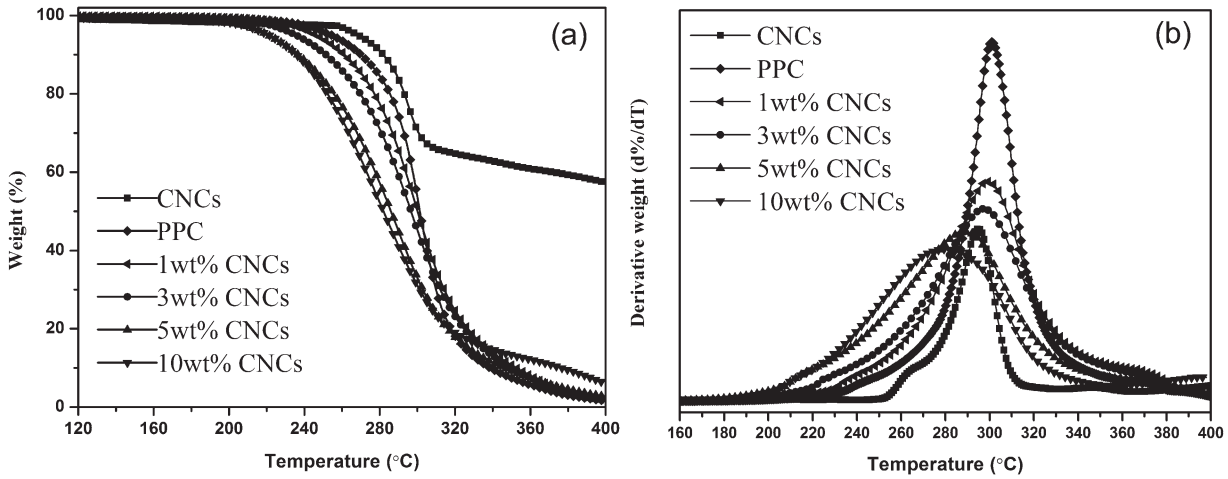

Figure 6. (a) TGA and (b) DTG curves of CNCs/PPC nanocomposites with various CNCs content.

The glass transition temperature (T_g) of the nanocomposites was detected on a differential scanning calorimeter (Netzsch204F1, Phoenix). The samples were heated to 120°C and stayed at 120°C for 5 min, then subsequently cooled to 0°C and heated again to 80°C at 10°C/min. The T_g was observed from the second heating scan.

The hydrophilicity of the nanocomposites was characterized by water contact angles on a Data physics OCA40 contact angle analyzer at room temperature. The water droplet (0.5 μL) delivered from a needle connected to a syringe pump and deposited on the surface. At least five independent determinations on different areas of each specimen were averaged.

RESULTS AND DISCUSSION

Morphologies and Dispersion of CNCs

In Figure 1, the rod-like CNCs were observed, and their width and length were about 10–15 nm and 200–400 nm, respectively. CNCs would be partially sulfate-functionalized during sulfuric acid hydrolysis of MCC. As this negatively charged sulfate ester moieties located on the surface of CNCs contributed to stabilizing the dispersion of CNCs by the electrostatic repulsion, the as-prepared aqueous suspension of CNCs [Figure 2(a)] could be stable for several weeks and no precipitation was observed. During the solvent exchange process, the strong interactions between CNCs and water were substituted by relative weaker interactions with acetone. This sol-gel process led to a transformation from colloid suspension of CNCs to macroscopic CNCs–acetone organogels [comprising 1.5 wt %, Figure 2(b)] which were similar with previous report.[24]

Figure 3 showed SEM images of fractured surface of CNCs/PPC nanocomposites with 1, 3, 5, 10 wt % of CNCs and pure PPC. It could be clearly observed that pure PPC looked different compared with the nanocomposites where tiny white dots appeared. These dots increased in quantity with the increase of CNCs content in the composites and these dots should be the transversal sections of CNCs embedded in polymer matrix. The micrographs illustrated these tiny white dots were homogeneously distributed and no aggregates were observed in the micrometer scale even when 10 wt % CNCs content was loaded, indicating that good dispersion of CNCs in PPC could be achieved using the sol-gel approach. Such well dispersion of the fillers was significant to the mechanical reinforcement of PPC.

Effects on the Glass Transition Temperature of PPC

The DSC curves of neat PPC and CNCs/PPC nanocomposites were shown in Figure 4.The neat PPC displayed a glass transition temperature at 34°C. As the amount of CNCs increased, the T_g of CNCs/PPC nanocomposites was elevated to 37.4°C when the CNCs content was 10 wt %, 3.4°C higher than that of neat PPC. This was ascribed to the restricted segmental motion of PPC molecular chains caused by the strong interaction between polymer matrix and the dispersed CNCs, especially the hydrogen bonding interactions between the abundant hydroxyl groups of CNCs and the carbonyl groups of PPC.[23,29]

It is worth noting that the T_g was increased by 1.5°C compared with neat PPC when the nanocomposites contained only 1 wt % of CNCs, however, as shown in Figure 5, that value was merely increased by 1.9°C as the CNCs content varied from

Table I. TGA and DTG Results of CNCs/PPC Nanocomposites

Materials	PPC	CNCs/PPC (1 wt %)	CNCs/PPC (3 wt %)	CNCs/PPC (5 wt %)	CNCs/PPC (10 wt %)	CNCs
$T_{d(5\%)}$ (°C)	254	246	235	220	221	268
T_{dmax} (°C)	300	299	297	290	281	294

$T_{d(5\%)}$ and T_{dmax} represent the temperature of thermal degradation for 5% weight loss and the temperature at maximum weight-loss rate.

Table II. The Mechanical Properties of CNCs/PPC Films

Materials	Yield strength (MPa)	Break elongation (%)	Young's modulus (MPa)
PPC	10.2	398	681
PPC/CNCs (1 wt %)	10.7	360	658
PPC/CNCs (3 wt %)	13.5	206	950
PPC/CNCs (5 wt %)	12.9	101	1043
PPC/CNCs (10 wt %)	21.0	78	1378

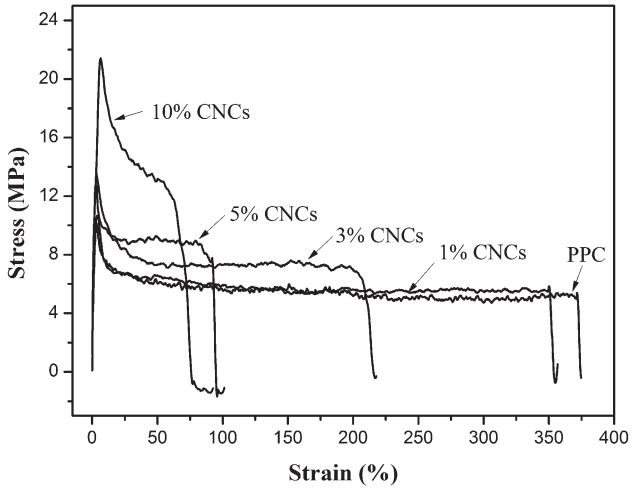

Figure 7. Typical stress–strain curves of neat PPC and its nanocomposites comprising 1, 3, 5, and 10 wt % CNCs.

1 to 10 wt %. This revealed that a small amount of stiff rod-shaped CNCs had been sufficient to reduce the free volume of PPC and thus inhibit its molecular mobility. CNCs reinforced PPC with glass transition temperature of 37.4°C which is closer to human body temperature may find potential application in biomedical fields.

Thermal Stability of CNCs/PPC Nanocomposites

Figure 6 showed the thermal degradation behaviors of pure CNCs, PPC, and CNCs/PPC nanocomposites with different CNCs content, and main thermal parameters were summarized in Table I. As shown in Figure 6 and Table I, $T_{d(5\%)}$ represents the onset temperature of thermal degradation for 5% weight loss, it was found that $T_{d(5\%)}$ gradually decreased from 254 to 220°C as CNCs content increased from 0 to 5 wt %, and no further obvious drop was observed when CNCs content exceed 5 wt %. It should be noted that the CNCs used in this work displayed an onset of degradation of 5% mass loss at 268°C, which was a little higher than pure PPC. However, TGA and DTG curves proved that CNCs led to lower thermal stability of PPC. This could be attributed to the introduction of thermo-sensitive sulfate groups generated on the surface of CNCs during sulfuric acid hydrolysis procedure.[30] Desulfation probably took place at lower temperature as the elimination of sulfuric acid in sulfated anhydroglucose required less energy,[31] as a result, sulfuric acid molecules were released and thus might accelerate the decomposition or depolymerization of PPC. Hence, weak thermal stability of the nanocomposites occurred. However, conversely, if CNCs with no or few residual acid groups, they always showed higher thermal stability.[31,32] Wang et al.[28] reported that, when desulfated CNCs were composited with PPC, the thermal degradation of CNCs/PPC nanocomposites would be suppressed by the strong interaction between CNCs and PPC.

Mechanical Properties of CNCs/PPC Nanocomposites

Yield strength and Young's modulus of CNCs/PPC films as representative mechanical properties were listed in Table II. Typical stress–strain curves of the nanocomposites were also shown in Figure 7 and it clearly showed that all samples yielded at quite low elongation. Obviously, the incorporation of CNCs took a profound impact on the mechanical performances of PPC. When CNCs content increased from 0 to 10 wt %, the yield strength and Young's modulus were drastically improved by 106% from 10.2 to 21.0 MPa and by 102% from 681 to

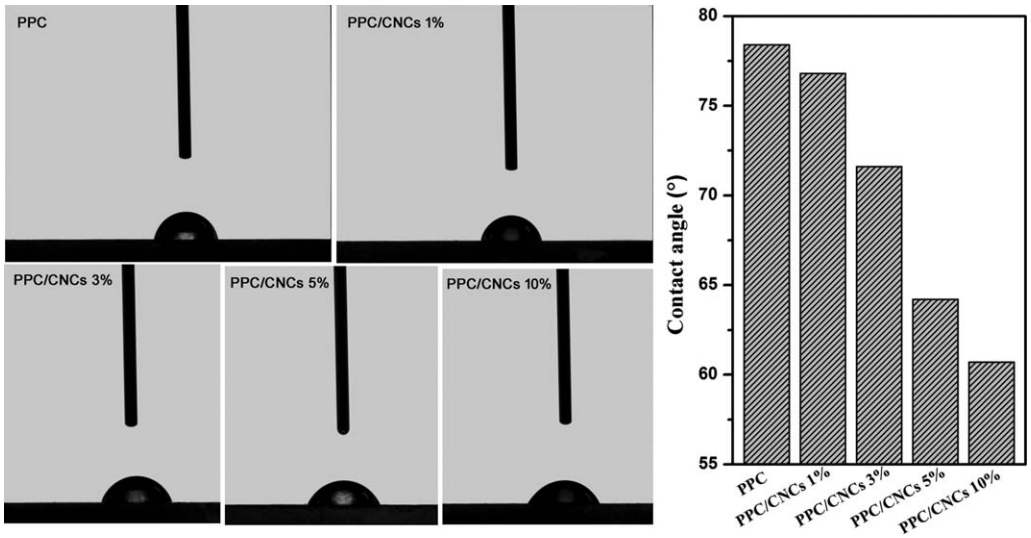

Figure 8. Water contact angle of CNCs/PPC nanocomposites comprising various CNCs content.

1378 MPa, respectively. This significant change of mechanical behavior could be understood using the percolation model of Ouali et al.[33] Presumably due to the hydrogen bonding of the surface hydroxyls, the rigid nanoparticle fillers strongly interacted with each other and formed a three-dimensional percolating network in the soft PPC matrix. Additionally, the interfacial interaction between CNCs and PPC facilitated the stress transferring from PPC matrix to the percolating rigid phase. It could be concluded that the strong filler–filler interactions together with the matrix–filler interactions contributed to the high yield strength and modulus. Meanwhile, the mobility of PPC polymer chains was weakened by the mutual attractive force between PPC macromolecules and the surrounded CNCs, therefore, elongation at break of the nanocomposites exhibited a steady decrease from 398 to 78% with the decreasing percentage of CNCs, demonstrating the strength and modulus of PPC were improved at the expense of losing toughness. However, more recently, Wang et al.[28] reported that PPC comprising 10 wt % CNCs showed a 1.3-fold increase in tensile strength without a marked decline of elongation at break compared with neat PPC using the re-dispersible powder as reinforcing material.

Water Contact Angle

It is qualitatively understood that cellulose is intrinsically hydrophilic. According to previous reports, for CNCs, the water contact angles were 11.5° for dry-cast CNCs films and 23.7° for spin-coated CNCs films.[34,35] As shown in Figure 8, the water contact angle continually decreased from 78.4° for neat PPC to 60.7° for the nanocomposites film containing the highest concentration of CNCs. Apparently, due to the hydroxyl groups available on the surface of CNCs which were generally regarded as the initial sites of water sorption, and the increased surface roughness induced by the introduction of CNCs, the surface wettability of PPC was improved. The phenomenon that polymers became more hydrophilic after incorporating with nanosized cellulose was also described in the literatures.[36,37] This implied that CNCs could be a candidate of reinforcing material which were able to achieve simultaneous improvement of mechanical properties and hydrophilicity. The improved hydrophilicity of PPC was beneficial to cellular adhesion and the improvement of biocompatibility, making it a kind of promising materials for tissue engineering.

CONCLUSIONS

CNCs/PPC nanocomposites were successfully prepared via a sol-gel process followed by solution casting. As a solvent exchange method, this sol-gel process was able to avoid the strong aggregation during the drying process of CNCs, and thus there would be no need of prolonged ultrasonication to redisperse the CNCs which caused their mechanical degradation. SEM observations verified well dispersion of CNCs in PPC matrix. The mechanical performances, thermal properties, and hydrophilicity of pure PPC and its nanocomposites containing 1, 3, 5, and 10 wt % of CNCs were examined. Since the formation of CNCs hydrogen bonded percolating network, the yield strength and Young's modulus of the nanocomposites were significantly improved from 10.2 to 21.0 MPa and from 681 to 1378 MPa, respectively. The T_g of PPC was raised from 34.0 to 37.4°C because of the restricted molecular mobility. However, the partially sulfated CNCs diminished the thermal stability of PPC. Interestingly, water contact angle measurements confirmed that PPC turned more hydrophilic by the inclusion of hydrophilic cellulose nanoparticles. The results of this work will have an important impact on expanding the practical application of PPC.

ACKNOWLEDGMENTS

This work was supported by Innovation Program of Shanghai Municipal Education No. 12ZZ062, the Fundamental Research Funds for the Central Universities, and Programme of Introducing Talents of Discipline to Universities No. 111-2-04.

REFERENCES

1. Moon, R. J.; Martini, A.; Nairn, J.; Simonsen, J.; Youngblood, J. *Chem. Soc. Rev.* **2011**, *40*, 3941.
2. Alina, S. *Prog. Polym. Sci.* **2011**, *36*, 1254.
3. Dong, Y.; Wang, X.; Zhao, X.; Wang, F. *Polym. Sci., Part A: Polym. Chem.* **2012**, *50*, 362.
4. Seo, J.; Jeon, G.; Jang, E. S.; Bahadar Khan, S.; Han, H. *J. Appl. Polym. Sci.* **2011**, *122*, 1101.
5. Yao, M.; Mai, F.; Deng, H.; Ning, N.; Wang, K.; Fu, Q. *J. Appl. Polym. Sci.* **2011**, *120*, 3565.
6. Yang, G.; Geng, C.; Su, J.; Yao, W.; Zhang, Q.; Fu, Q. *Compos. Sci. Technol.* **2013**, *87*, 196.
7. Bian, J.; Wei, X. W.; Gong, S. J.; Zhang, H.; Guan, Z. P. *J. Appl. Polym. Sci.* **2012**, *123*, 2743.
8. Gao, J.; Chen, F.; Wang, K.; Deng, H.; Zhang, Q.; Bai, H.; Fu, Q. *J. Mater. Chem.* **2011**, *21*, 17627.
9. Shi, X.; Gan, Z. *Eur. Polym. J.* **2007**, *43*, 4852.
10. Chen, W.; Pang, M.; Xiao, M.; Wang, S.; Wen, L.; Meng, Y. *J. Reinf. Plast. Compos.* **2010**, *29*, 1545.
11. Lin, N.; Chen, G.; Huang, J.; Dufresne, A.; Chang, P. R. *J. Appl. Polym. Sci.* **2009**, *113*, 3417.
12. Siqueira, G.; Mathew, A. P.; Oksman, K. *Compos. Sci. Technol.* **2011**, *71*, 1886.
13. Blachechen, L.; Mesquita, J.; Paula, E.; Pereira, F.; Petri, D. S. *Cellulose* **2013**, *1*.
14. Lin, N.; Yu, J. H.; Chang, P. R.; Li, J. L.; Huang, J. *Polym. Compos.* **2011**, *32*, 472.
15. Jalal Uddin, A.; Araki, J.; Gotoh, Y. *Biomacromolecules* **2011**, *12*, 617.
16. Yu, H. Y.; Qin, Z. Y.; Liu, Y. N.; Chen, L.; Liu, N.; Zhou, Z. *Carbohydr. Polym.* **2012**, *89*, 971.
17. Zhu, Y.; Hu, J.; Luo, H.; Young, R. J.; Deng, L.; Zhang, S.; Fan, Y.; Ye, G. *Soft Matter* **2012**, *8*, 2509.
18. Huq, T.; Salmieri, S.; Khan, A.; Khan, R. A.; Le Tien, C.; Riedl, B.; Fraschini, C.; Bouchard, J.; Uribe-Calderon, J.; Kamal, M. R.; Lacroix, M. *Carbohydr. Polym.* **2012**, *90*, 1757.
19. Azizi Samir, M. A. S.; Alloin, F.; Sanchez, J.-Y.; El Kissi, N.; Dufresne, A. *Macromolecules* **2004**, *37*, 1386.

20. Viet, D.; Beck-Candanedo, S.; Gray, D. *Cellulose* **2007**, *14*, 109.
21. van den Berg, O.; Capadona, J. R.; Weder, C. *Biomacromolecules* **2007**, *8*, 1353.
22. Favier, V.; Cavaille, J. Y.; Canova, G. R.; Shrivastava, S. C. *Polym. Eng. Sci.* **1997**, *37*, 1732.
23. Dong, H.; Strawhecker, K. E.; Snyder, J. F.; Orlicki, J. A.; Reiner, R. S.; Rudie, A. W. *Carbohydr. Polym.* **2012**, *87*, 2488.
24. Capadona, J. R.; Van Den Berg, O.; Capadona, L. A.; Schroeter, M.; Rowan, S. J.; Tyler, D. J.; Weder, C. *Nat. Nanotechnol.* **2007**, *2*, 765.
25. Missoum, K.; Bras, J.; Belgacem, M. *Cellulose* **2012**, *19*, 1957.
26. Tang, L.; Weder, C. *ACS Appl. Mater. Interfaces* **2010**, *2*, 1073.
27. Hu, X.; Xu, C.; Gao, J.; Yang, G.; Geng, C.; Chen, F.; Fu, Q. *Compos. Sci. Technol.* **2013**, *78*, 63.
28. Wang, D.; Yu, J.; Zhang, J.; He, J.; Zhang, J. *Compos. Sci. Technol.* **2013**, *85*, 83.
29. Littunen, K.; Hippi, U.; Saarinen, T.; Seppala, J. *Carbohydr. Polym.* **2013**, *91*, 183.
30. Wang, N.; Ding, E.; Cheng, R. *Polymer* **2007**, *48*, 3486.
31. Roman, M.; Winter, W. T. *Biomacromolecules* **2004**, *5*, 1671.
32. Yu, H.; Qin, Z.; Liang, B.; Liu, N.; Zhou, Z.; Chen, L. *J. Mater. Chem. A* **2013**, *1*, 3938.
33. Ouali, N.; Cavaille, J. Y.; Perez, J. *Rubber Compos. Process. Appl.* **1991**, *16*, 55.
34. Aulin, C.; Ahok, S.; Josefsson, P.; Nishino, T.; Hirose, Y.; Österberg, M.; Wågberg, L. *Langmuir* **2009**, *25*, 7675.
35. Yamane, C.; Aoyagi, T.; Ago, M.; Sato, K.; Okajima, K.; Takahashi, T. *Polym. J.* **2006**, *38*, 819.
36. Yu, H. Y.; Qin, Z. Y.; Zhou, Z. *Prog. Nat. Sci.* **2011**, *21*, 478.
37. Ago, M.; Jakes, J. E.; Johansson, L.-S.; Park, S.; Rojas, O. *J. ACS Appl. Mater. Interfaces* **2012**, *4*, 6849.